Lunar Sentinel - Guardian that watches over lunar landings

Prof. (Dr.) Hrishikesh Joshi
Dept. of Artificial Intelligence & Data Science (AI&DS)
Vishwakarma Institute of Technology, Pune, India
hrishikesh.joshi@vit.edu

Prerna Shitole
Dept. of AI & DS
VIT Pune
prerna.shitole24@vit.edu

Swara Shetye
Dept. of AI & DS
VIT Pune
shetye.swara01@gmail.com

Ashish Tadavi
Dept. of AI & DS
VIT Pune
ashish.tadavi24@vit.edu

Prajakta Vetale
Dept. of AI & DS
VIT Pune
prajakta.vetale24@vit.edu

Engineering Design and Innovation (EDAI)
Vishwakarma Institute of Technology, Pune, 411037, Maharashtra, India

Abstract—A safe lunar landing on moon requires precise identification of terrain hazard particularly regions having craters, steep slopes, shadows and high terrain roughness. These hazards can be critical to land on and can cause trouble for rover mobility post landing operations and research. In this we used Chandrayaan 2 TMC-2 imagery and Digital Elevation Model datasets to detect terrain hazards and find a quantitative lunar surface safety site. From DEM dataset parameters like slope gradient, terrain roughness and elevation were derived successfully while from TMC-2 imagery shadow and texture information were extracted. For a safe landing in high risk area we developed an AI base system that automatically detects safe areas and calculates a LSI(landing safety index) that gives safety score where higher the LSI values indicate flat, well illuminated and row roughness areas which are suitable for landing or rover mobility. The LSI map classifies the surface into safe, moderate and high risk zones identifying craters, shadowed depressions and roughness specified as unsafe areas for landing. This approach is structured as well as data driven method for evaluating safe lunar sites using input devices and it can also support future landing site selection, rover path plannings and a successful lunar landing.

Index Terms—lunar lander, landslide, hazard detection, deep learning, thermal map, satellite pictures.

I. Introduction

Before exploration of the moon, it demands accurate analysis of surface risks conditions even selecting a landing site or post landing rover route defining. Lunar terrain are uneven and highly irregular due to impact of various events occurred over a course of billion years and moon has absence of atmosphere on it. One of the most dominant geological features on the moon is crater which are formed when a meteoroid hits or strikes the surface of the moon at high velocity. Craters are found in various sizes from microscopic to hundreds of kilometer wide. Every crater has steep rims, uneven crater floors, loose regolith and rocky ejecta material scattered around the perimeter. These characteristics make the landing conditions risky and they may even do structural damage. Similarly rover mobility may be limited due to steep surfaces or loose terrain. More challenges affecting landing safety are shadow and illumination. Since the moon does not have atmosphere, shadows are sharp and persistent which makes the navigation difficult and it reduces solar panel efficiency. Areas having strong illumination may also hide small obstacles or slopes that could be miscalculated due to sensors. Additionally terrain roughness which is elevation of the surface within local neighborhoods states how stable the surface is for hardware deployment. Due to these conditions and constraints identifying locations with optimal slope, efficient illumination and terrain smoothness becomes essential for planning of the mission. Remote sensing is a reliable tool to evaluate the given parameters for landing. Chandrayaan 2 contributes high resolution TMC-2 imagery and from DEM data measurable terrain indicators required for hazard assessment were extracted. In our study a structured approach is used to process Chandrayaan 2 dataset and derive multiple characteristics like slope, roughness, shadows and surface texture. These are then normalized and combined using weighted hazard fusion methodology to calculate Landing Safety Index (LSI). The LSI is a continuous scale classifying sites into safe, moderate and hazardous regions. The output maps highlight dangerous crater rims, high shadowed depression, steep slopes and rough ejecta blankets while also looking for flat and well-illuminated terrain which favor our spacecraft landing and post landing rover operations. This methodology provides a transparent, well structured and a framework that evaluates landing safety sites using remote sensing data and supports decision making for our future lunar missions.

II. Literature Review

1) This research paper focuses on how landslides are detected inside its impact craters. Traditionally the land-

slides were detected visually looking at images but, in this paper, mathematical and automated methods that are DEM (Digital Elevation Models) and Chebyshev polynomial are implemented. They can analyze and detect asymmetrical crater walls which are likely due to landslides. The method successfully was able to detect landslides in Cassini A crater [1].

2) This research paper focuses on landslides in lunar impact craters as well and an automatic and objective method that automatically detects landslides specifically slumps inside craters using Chebyshev polynomial interpolation of craters cross section of global DEMs. It used two approaches: Empirical Absolute Thresholding and Statical Adaptive Threshold. It was applied to 204 impact craters [2].
3) This project focuses on using deep convolutional neural networks and not traditional mathematical algorithms for studying the automated identification of lunar craters. The CNN identifies geological history, surface evolution, and landing site selection for lunar missions. Traditional methods were time consuming and using neural networks is more accurate and faster. The CNN and U-Net model with ResNet18 was used for image segmentation and reorganization of Chandrayaan-2's data [3].
4) This research paper focuses on crater identification and age estimation using transfer learning. It uses DOM (Digital Orthophoto Maps) and DEM. A two staged pipeline was deployed training using CE-1 data then transferred the trained model to CE-2 data. Age estimation was also implemented via ensemble transfer learning. Two staged classification models were developed with CNN and ensemble learning via genetic algorithm-based weighting. Estimated 109,956 new craters were identified, and 18,996 craters were assigned ages [4].
5) This research paper focuses on evaluation of landing site under moonquakes and meteorite Impacts in Taurus-Littrow Valley (TLV) for Apollo 17 landing. 2D seismic site evaluation was initialized and how it affects ground motion amplification and wave scattering. Hence, it proved how important it is to evaluate sites with seismic evaluations for future lunar landings [5].
6) This research paper focuses on landing orbiters, rovers and landers on the south region of the moon and selecting safe and scientifically valuable landing sites is valuable for mission success. Constraints followed were slopes $< 15^{\circ}$, boulders $<$ 0.5m and crater density in safe limits. Sunlight received 14 days after landing and continuous earth communication. Out of the sites SLS-54 prime site and ALS-01 alternative sites were chosen for scientists' interest. So, all the work was done using engineering safety constraints and science interests using datasets and sources [6].
7) JAXA's Smart Lander for Investigating Moon used OHRC and mapped meter sized boulders and identified boulders trail of how the surrounding impacted the trail. Spatial distribution analysis was implemented that crater areas were divided into 18 angular sectors, and rose diagrams were visualized. Also measured how the boulder falls with radial distance from the center of the crater. Mapping boulders helped landers identify touchdown sites more efficiently. The mission helped identify 15k+ boulders and mapping landing hazard regions for future lunar missions [7].
8) Previous paper studied that lunar boulder distribution has relied highly on images from the Lunar Reconnaissance Orbiter Camera (LROC) its Narrow Angle Camera (NAC) offered a resolution sufficient to detect boulders larger than 2m. These showed empirical relationships between boulder size, crater age, power law function was used to describe fragmentation and ejection processes. But it limited spatial resolution of previous datasets that restricted detection of smaller boulders, and these were observed data which struggled to adapt to new or unexpected situations when aroused that hindered refinement of the empirical models. To overcome the limitations this paper provides an unprecedented sub-meter resolution (0.25m) imagery, allowing Identification of boulders below one meter in size. Their paper mapped more than 2000 boulders around Boguslawsky E as a young crater and analyzed spatial, size frequency, and directional distributions. Apart from the single fragmentation of power law, the authors applied both power law and Weibull distribution offered a superior representation (R^2 = 0.99), implying sequential fragmentation of ejected material. Through empirical age relations proposed by Watkins et al. (2019) and Li et al. (2018), they estimated the crater's age to be between 50 and 90 Ma [8].
9) This paper focuses on the identification of impact craters to understand the geographical history and evolution of solar planetary bodies. Traditional detection methods were based on image processing techniques like Hough Transform, watershed segmentation, and edge detection which struggled with low accuracy and adaptability due to light variations, overlapping of craters, and scale diversity. Due to advancement in technology of AI and Computer Vision, the focus has been shifted to Deep Learning models for robust crater recognition. Earlier models such as DeepMoon and DeepMars applied convolutional neural networks (CNNs) for crater detection on lunar and Martian surfaces, showed improved precision over traditional algorithms but these models are heavily dependent on annotated datasets and weak in generalization. A segmentation model was built combining U-Net architecture with a ResNet-18 to train Chandrayaan-2 Terrain Mapping Camera-2 (TMC-2) data to help models learn faster and produce clear and more precise crater [9].
10) A challenge in studying lunar geomorphology is accurate recognition of landslides within impact craters. Earlier studies relied on visual inspection of optical images and digital elevation models (DEMs) which led to subjective and inconsistent classification. In 2018 to

overcome this, a semi-automated method to detect lunar landslides using Chebyshev polynomial interpolation of craters cross sections was derived from global lunar DEM's. This approach was used to analyze symmetry in craters for identification of slumps in simple, bowl-shapes. These two recognition criteria were compared EAT (empirical absolute threshold) and SAT (statistical adaptive thresholding with results leaning on EAT methods side with higher accuracy for recognizing cross sectional asymmetries related to landslides. The paper analyzed 204 crater profiles and achieved 92.8% success classifications [10].

11) This paper focuses on improving automated crater and boulder detection on Moon's surface using deep learning models. The goal of the paper is to study lunar surface mapping faster, which is more accurate and is not dependent on manual mapping. Craters and boulder identification are important assessments in lunar exploration since it helps researchers understand history, geographical activity on moon as well as surface hazard for future missions. Previously studies were highly dependent on manual inspection of high-resolution lunar dataset or traditional image processing like edge detection and thresholding. All methods are slow, inconsistent, and highly affected by lightning variations, overlapped craters, and surface noise. To overcome these limitations, the paper introduced a hybrid AI model combining Convolutional Neural Networks (CNN) and YOLOv8 for faster and more precise crater and boulder detection [11].
12) This paper focuses on identifying safe and possible landing sites for the Chandrayaan-2 Lander in the southern hemisphere of the moon between 65° S and 90° S latitude. The goal was to find a site that met both engineering (safe, stable and visible from earth) as well as scientific goals for studying geological terrain and composition of soil. The success of safe site landings depends on choosing a hazard free site which doesn't have steep slopes, large boulders and long shadows while getting sunlight for power and line of sight for communication. During Chandrayaan-1 studies focused on sites near 85°−90° degree latitudes, where sunlight is almost continuing. These sites had operations difficulties like extreme local slopes, etc. made rover operations difficult. To overcome these challenges, the search area was extended to 65°−90° S latitude on Moon. A multi-criteria hazard analysis of optical images and DEM's was combined. Using multiple datasets, they derived slope mapping and shadow maps [12].

III. Methodology

The project workflow represents a method to systematically identify and evaluate safe lunar landing zones by combining image data from Chandrayaan-2 Terrain Mapping Camera (TMC-2) with the Digital Elevation Models (DEMs) and craters detected in LROC NAC images using the YOLOV8 model training. The approach focuses on terrain characterisation (terrain norm analysis), slope-derived hazard estimate and crater distribution analysis to produce an integrated landing safety index map (LSI) surface, following standard practices in planetary landing hazard assessment [15], [18]. The complete workflow was carefully constructed to ensure that spatial consistency and analytical robustness are preserved across all used datasets.

A. Data Acquirement and Description

For data acquisition, high-resolution lunar surface datasets from Chandrayaan-2 TMC-2 (Level-2) were used as the primary source. These orthorectified panchromatic strips provide clean, geometrically corrected surface imagery, suitable for analysing terrain conditions. The accompanying TMC-2 DEM enables the extraction of elevation-based terrain metrics, such as slope and hillshade, which are essential for assessing the stability of potential landing sites [13].

Additionally, LROC Narrow Angle Camera (NAC) images were used. These images are extremely useful for identifying surface craters, which is one of the most common hazards faced during lunar landings due to steep rims, ejecta blocks, and uneven interiors. Craters were manually annotated to create a ground-truth crater layer for training YOLOv8 crater detection model following recommendations from crater-mapping studies in lunar surface analysis [15], that will be implemented into the hazard model later.

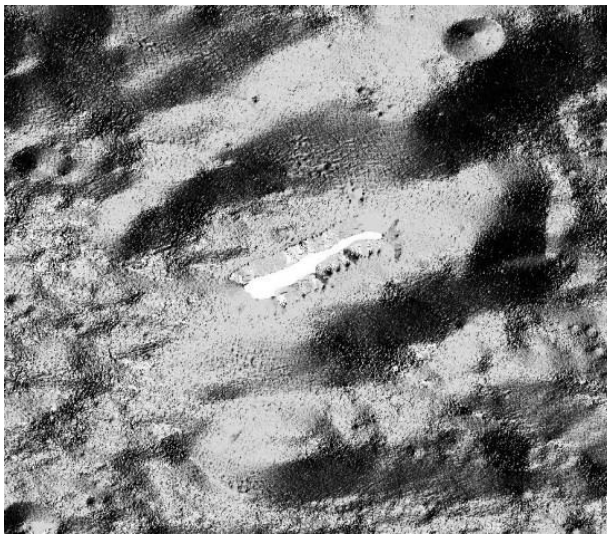

Fig. 1. Chandrayaan-2 TMC-2 lunar surface image layer representing the region selected for landing hazard assessment. Source: issdc.gov.in

B. Geospatial Preprocessing and Terrain Parameter Derivation

To ensure that all datasets align correctly over the lunar surface, the Chandrayaan-2 TMC-2 imagery and DEMs were first projected into a common lunar selenographic coordinate system. Using QGIS Developers Tools and GDAL utilities, each dataset was clipped to the selected Region of Interest (ROI) and resampled to maintain a uniform spatial resolution.

This standardization ensures that every pixel corresponds to the same physical ground distance, allowing terrain parameters to be compared and combined reliably, as recommended in DEM-based terrain studies [13].

C. Terrain Slope Derivation

The terrain slope was calculated from the DEM using the classical surface gradient formulation, widely documented in digital terrain analysis literature [13]:

$$S(x,y) = \sqrt{\left(\frac{\partial z}{\partial x}\right)^2 + \left(\frac{\partial z}{\partial y}\right)^2} \quad (1)$$

Here, $z(x, y)$ represents the elevation at each pixel. This slope layer highlights steep terrain such as crater rims, inner walls, and ejecta boundaries areas generally unsafe for lander footpad stability. $\frac{\partial z}{\partial x}$, $\frac{\partial z}{\partial y}$ are partial derivatives computed using a 3×3 neighbourhood kernel.

D. Slope Surface Normalization

Since slope values vary significantly across the lunar terrain, a min-max normalization approach, following the common normalization strategy described by Jain et al. (2000) for multi-criteria raster integration [13]:

$$S_{norm}(x, y) = \frac{S(x,y) - S_{min}}{S_{max} - S_{min}} \quad (2)$$

This process of normalization places all slope values within the range 0-1, enabling them to be directly integrated with other hazard components such as shadows and crater density during the risk-mapping stage.

Fig. 2 shows the slope-enhanced lunar surface derived from the Chandrayaan-2 DEM using QGIS. A pseudocolor scheme has been applied where:

- Bright cyan, green, and yellow tones denote steep terrain such as crater rims, inner walls, and highly fractured ejecta layers.
- Deep blue regions correspond to relatively flat and stable surfaces that are more favorable for safe lander touch-down.
- The concentric and radial patterns around large craters clearly depict the structural morphology of impact basins.
- Numerous micro-craters and subtle undulations become visually prominent due to the slope enhancement.

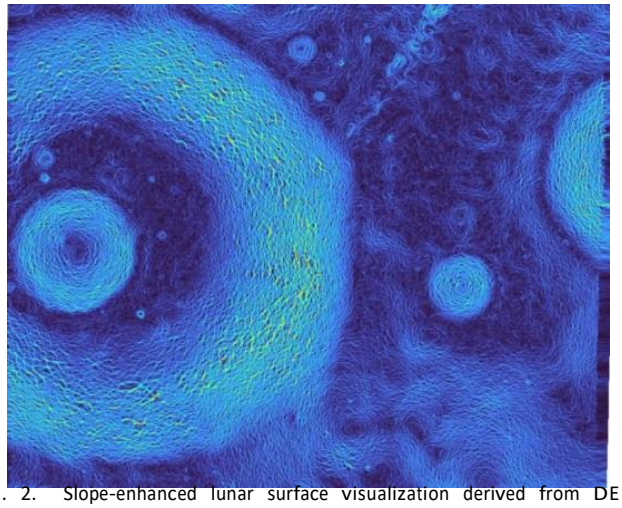

Fig. 2. Slope-enhanced lunar surface visualization derived from DEM processing in QGIS.

E. Hillshade Generation for Illumination Analysis

A hillshade raster was created from the DEM to simulate solar illumination on the lunar surface. This step follows the classical illumination modeling approach described by Horn (1981) [14].

Hillshade identifies regions, where navigation cameras can operate reliably and Shadowed regions, which may block terrain hazards and degrade performance of optical hazard detection systems during descent. These shadow-intense areas are later treated as high-risk in the hazard mode.

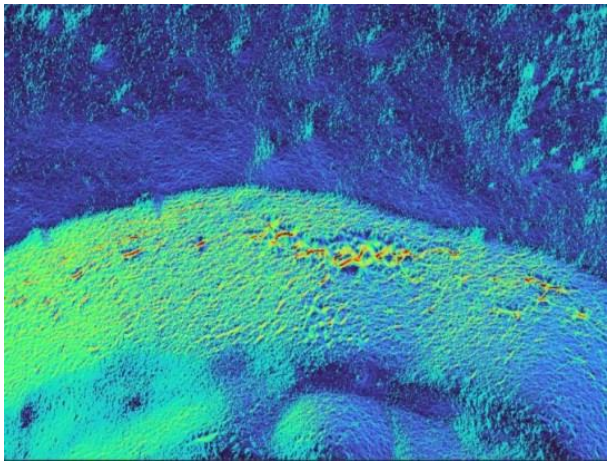

Fig. 3. Hillshade-Derived Illumination Map

Fig. 3 presents the hillshade raster generated from the DEM using the standard illumination model described by Horn (1981) [14]. The simulation incorporates a solar elevation angle of 45° and an azimuth angle of 315°, representing typical near-terminator lighting conditions encountered during lunar descent operations. Bright pixels correspond to well-illuminated terrain with high reflectance and good visual clarity, while darker pixels represent shadowed zones cast

by crater rims, interior walls, and elevated ridges. These persistent shadow regions constitute high-risk areas due to the degradation of optical contrast.

F. Crater Identification and Annotation Using LROC Imagery

Crater detection was performed using high-resolution LROC NAC imagery, where a custom-trained YOLOv8 object detection model was used to automatically identify crater rims, shadow regions, and ejecta boundaries. The training dataset consisted of manually labelled crater bounding boxes prepared from representative NAC image tiles. After training, the YOLOv8 model provided pixel-level crater localization with high confidence scores, enabling consistent and automated detection across the study area. Automated crater detection is consistent with modern machine-learning approaches for lunar hazard mapping, which improve crater localization efficiency compared to manual interpretation [15]. Resulted crater detections were converted into crater density raster for hazard analysis.

G. Hazard Surface Construction

Three key hazard components were derived to characterize lunar surface risk: Normalized slope (0-1 scale), Crater density surface, Illumination shadow mask. Shadow mapping was performed using a hillshade intensity threshold to identify regions experiencing persistent low illumination. Such regions are considered hazardous because visual sensors and surface-based perception systems become less reliable under low-contrast conditions [15]. All hazard layers were aligned in the same spatial reference frame and resampled to a uniform resolution. Each layer was then combined to produce an integrated hazard representation, following multi-criteria lunar landing safety frameworks recommended in prior research [16].

H. Landing Safety Index (LSI) Mapping

The Landing Safety Index (LSI) is a combined measure used to evaluate how safe each location is for a spacecraft to land. Instead of relying on a single parameter, the LSI integrates three major hazard factors: terrain slope, surface shadowing, and crater density. This approach aligns with established lunar terrain-hazard assessment models where multiple surface hazards are merged to evaluate safe touchdown zones [15], [16]. Each of these components influences landing safety differently: steep slopes affect the lander's balance, shadowed regions reduce visibility for onboard cameras, and crater-rich surfaces increase the risk of uneven or unstable contact.

To generate the LSI map, each hazard layer was first normalized and then merged using a weighted approach, where slope was given the highest significance, followed by illumination quality and crater density, in accordance with previous lunar terrain safety studies [15], [16]. YOLOv8-based crater detection contributed to the crater density layer, while hillshade analysis provided information on illumination shadows.

The final LSI map was categorized into three practical classes to support mission planning:

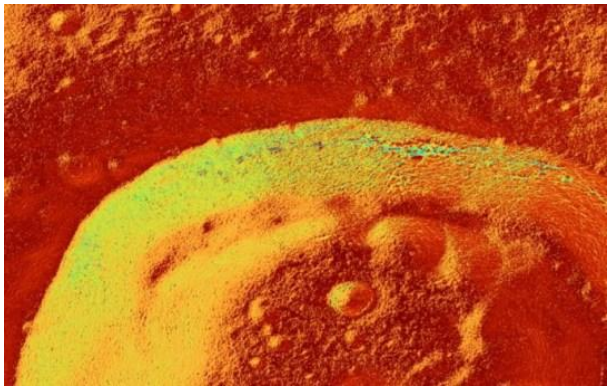

Fig. 4. LSI Map in QGIS

1) Safe zones (LSI > 0.8): These areas exhibit low hazard influence and offer stable conditions for landing. (Red zone)
2) Moderate-risk zones (0.5-0.8): These regions are acceptable but may require additional checks or mission constraints. (Yellow Zone)
3) High-risk zones (LSI < 0.5): These locations contain significant hazards such as steep slopes, persistent shadows, or high crater roughness and are avoided for landing operations. (Blue zone)

This classification framework enables clear visualization of terrain safety and helps mission teams identify the most suitable and reliable landing site candidates.

IV. Results and Discussions

The proposed lunar hazard detection and visualization system produced encouraging results when applied to multi-source lunar datasets. The system was able to automatically detect and map critical surface hazards such as boulders, craters, slopes, and thermal anomalies, all of which pose significant challenges for landing site selection. The YOLO-based object detection model consistently identified boulders of varying sizes and provided a reliable estimate of their spatial distribution, which is a key factor in assessing landing safety. At the same time, slope and elevation analysis derived from DEMs successfully highlighted regions with steep gradients and unstable terrain that could compromise lander stability. The use of Diviner thermal data further strengthened the analysis by revealing thermal anomalies and areas of unstable regolith, which are not easily detected through visual imagery alone. By integrating all hazard layers, the system generated a composite Hazard Index that provided a unified measure of surface risk. This Hazard Index enabled the classification of the lunar surface into three distinct categories: safe zones with relatively flat and stable terrain, moderate risk zones with partial hazards, and highly hazardous zones with multiple risk factors combined. The classification maps created through this process offered a clear and comprehensive representation of the spatial distribution of hazards, thus providing a more reliable framework for selecting landing sites. In addition to

hazard detection and classification, the development of an interactive web-based dashboard significantly enhanced the usability of the system. The dashboard allowed for dynamic visualization of hazard maps, layer selection, and radar-inspired alerts, enabling users to assess landing sites in real time. Evaluation using representative lunar datasets confirmed that the system not only improved accuracy in hazard detection but also increased the speed and efficiency of decision-making compared to conventional DEM-only analyses. These results strongly suggest that the integration of multi-source data with AI-driven feature extraction represents a substantial improvement in lunar hazard assessment.

V. Conclusion

This research demonstrates a comprehensive and reliable methodology for lunar hazard detection and visualization by combining satellite imagery, thermal data, and elevation models with advanced feature extraction techniques. The results indicate that the system successfully identified and classified hazardous regions on the lunar surface, providing a practical solution for safe landing site selection. By leveraging AI-powered boulder detection, DEM-based slope analysis, and thermal anomaly mapping, the system delivered a more robust assessment of lunar terrain hazards compared to traditional methods that rely on a single dataset. The redundancy of results across multiple hazard layers reinforces the accuracy of the findings, as hazardous regions identified by one dataset were often confirmed by others, thereby increasing confidence in the system's classifications. The creation of a composite Hazard Index proved effective in simplifying complex multi-source data into a clear and actionable framework, while the interactive dashboard provided an intuitive tool for mission planners to visualize and interpret hazard zones in real time. In conclusion, the study highlights the potential of multi-source data fusion and AI-based analysis in advancing planetary hazard detection. The system not only enhances automation but also ensures safer and more efficient landing site selection. Looking forward, this framework can be extended for real-time onboard processing during lunar landings, integrated with data from future missions such as Chandrayaan-3, and adapted to support exploration in Mars-like environments. Such advancements will significantly contribute to the safety, reliability, and overall success of upcoming planetary exploration missions.

VI. Future Scope

Future scope would be detecting craters and then adding all the thinks in the dashboard with the help of this also next would be to integrate a camera to get images or footage slips from the lander so it can respond it and visualize the output to help safe landing.

One important next step in this work is to add a Crater Risk Index (CRI). The current system is mostly focused on finding surface hazards like boulders and landslides. However, craters are still very important for finding safe landing zones. The framework could give various crater regions different risk values by connecting discoveries to a CRI map made from high-resolution lunar inclination models. This would enable the visualizer show what the camera sees at that time and consider into consideration the fundamental terrain characteristics, that would make the safety assessment more precise and reliable.

In future we can work on integrating a high-resolution camera that is integrated with ai that can detect safe landing zone and prevent hazard landing zones on moon. A high-resolution camera that provides the needed spatial details and demonstrates Ai-assisted hazard free detection with datasets that shows on board real-time inference and sub-decision making during the final descent phase of the lunar rover.

Acknowledgment

The authors express their heartfelt gratitude to our guiding faculty Prof. Hrishikesh Joshi Sir for providing assistance in making of our model and answering our queries.

References

[1] V. Yordanov, M. Scaioni, M. Brunetti, M. Melis, A. Zinzi, and P. Giommi, "Mapping landslides in lunar impact craters using Chebyshev polynomials and DEM's," ISPRS International Archives of the Photogrammetry, Remote Sensing and Spatial Information Sciences, vol. XLI-B6, pp. 17–24, 2016.

[2] M. Scaioni, V. Yordanov, M. T. Brunetti, M. T. Melis, A. Zinzi, Z. Kang, and P. Giommi, "Recognition of landslides in lunar impact craters," European Journal of Remote Sensing, vol. 51, no. 1, pp. 47–61, Jan. 2018.

[3] M. Sinha, S. Paul, M. Ghosh, S. N. Mohanty, and R. M. Pattanayak, "Automated lunar crater identification with Chandrayaan-2 TMC-2 images using deep convolutional neural networks," Scientific Reports, vol. 14, no. 8231, pp. 1–13, 2024.

[4] C. Yang, H. Zhao, L. Bruzzone, J. A. Benediktsson, Y. Liang, B. Liu, X. Zeng, R. Guan, C. Li, and Z. Ouyang, "Lunar impact crater identification and age estimation with Chang'E data by deep and transfer learning," Nature Communications, vol. 11, art. no. 6358, 2020.

[5] H. Seifamiri, P. Maghoul, R. Boudreault, and A. M. Jablonski, "Seismic evaluation of Apollo 17 landing site against moonquakes and meteorite impacts," in Proc. ANGSA Apollo 17 – Crustal Processes, 2022, paper no. 2049.

[6] S. Amitabh, K. Suresh, and T. P. Srinivasan, "Potential landing sites for Chandrayaan-2 lander in Southern Hemisphere of Moon," in Proc. 49th Annual Lunar and Planetary Science Conference, Mar. 2018.

[7] R. R. Nagori, A. K. Dagar, and P. R. Rudravaram, "Boulders distribution at the proposed SLIM landing site near Shioli crater," in Proc. 55th Lunar and Planetary Science Conference, Houston, USA, Mar. 2024.

[8] A. K. Dagar, R. P. Rajasekhar, and R. Nagori, "Analysis of boulders population around a young crater using very high-resolution image of Orbiter High Resolution Camera (OHRC) on board Chandrayaan-2 mission," Icarus, vol. 386, p. 115168, 2022.

[9] Sinha, S. Paul, M. Ghosh, S. N. Mohanty, and R. M. Pattanayak, "Automated Lunar Crater Identification with Chandrayaan-2 TMC-2 Images using Deep Convolutional Neural Networks," Scientific Reports, vol. 14, no. 8231, pp. 1–23, 2024.

[10] M. Scaioni, V. Yordanov, M. T. Brunetti, M. T. Melis, A. Zinzi, Z. Kang, and P. Giommi, "Recognition of landslides in lunar impact craters," European Journal of Remote Sensing, vol. 51, no. 1, pp. 47–61, 2018.

[11] D. A. Gaikwad, V. Shirpurkar, N. Todkar, Z. Sutar, V. Salunkhe, and V. Madane, "Advanced Crater and Boulder Detection in Lunar Exploration with CNN and YOLO," International Journal of Scientific Research in Engineering and Management (IJSREM), vol. 9, no. 6, pp. 1–3, Jun. 2025.

[12] A. Amitabh and T. P. Srinivasan, "Potential Landing Sites for Chandrayaan-2 Lander in Southern Hemisphere of Moon," in 49th Lunar and Planetary Science Conference, LPI Contribution No. 2083, 2018.

[13] D. M. Mark, "Geographical information processing and applications," in Manual of Remote Sensing, vol. 1, 2nd ed., F. F. Sabins, Ed. Falls Church, VA, USA: American Society of Photogrammetry, 1987, pp. 631–711.

[14] B. K. P. Horn, “Hill shading and the reflectance map,” Proc. IEEE, vol. 69, no. 1, pp. 14–47, Jan. 1981.
[15] T. R. Smith, J. H. Roberts, and P. Lee, “Terrain hazard assessment and illuminated landing zone analysis for planetary landing missions,” Planet. Space Sci., vol. 89, pp. 1–13, Aug. 2013.
[16] A. Rangarajan, S. Mahanti, and K. Krishnan, “Integrated terrain hazard indexing for autonomous lunar landing using multi-parameter surface analysis,” Acta Astronaut., vol. 180, pp. 10–25, Mar. 2021.